J|A|C|S ARTICLES

Published on Web 06/02/2009

Copper-Responsive Magnetic Resonance Imaging Contrast Agents

Emily L. Que,[†] Eliana Gianolio,[||] Suzanne L. Baker,[§] Audrey P. Wong,[†] Silvio Aime,[||] and Christopher J. Chang*[,†,‡]

Department of Chemistry and Howard Hughes Medical Institute, University of California, Berkeley, California 94720, Center for Functional Imaging, Lawrence Berkeley National Laboratory, Berkeley, California 94720, and Centro di Biotechnologie Molecolari, University of Torino, Torino I-10125, Italy

Received February 9, 2009; E-mail: chrischang@berkeley.edu

Abstract: The design, synthesis, and evaluation of the Copper-Gad (CG) family, a new class of copper-activated magnetic resonance imaging (MRI) contrast agents, are presented. These indicators comprise a Gd^{3+}−DO3A core coupled to various thioether-rich receptors for copper-induced relaxivity switching. In the absence of copper ions, inner-sphere water binding to the Gd^{3+} chelate is restricted, resulting in low longitudinal relaxivity values ($r_1 = 1.2-2.2$ mM^{-1} s^{-1} measured at 60 MHz). Addition of Cu^+ to CG2, CG3, CG4, and CG5 and either Cu^+ or Cu^{2+} to CG6 triggers marked enhancements in relaxivity ($r_1 = 2.3-6.9$ mM^{-1} s^{-1}). CG2 and CG3 exhibit the greatest turn-on responses, going from $r_1 = 1.5$ mM^{-1} s^{-1} in the absence of Cu^+ to $r_1 = 6.9$ mM^{-1} s^{-1} upon Cu^+ binding (a 360% increase). The CG sensors are highly selective for Cu^+ and/or Cu^{2+} over competing metal ions at cellular concentrations, including Zn^{2+} at 10-fold higher concentrations. ^{17}O NMR dysprosium-induced shift and nuclear magnetic relaxation dispersion measurements support a mechanism in which copper-induced changes in the coordination environment of the Gd^{3+} core result in increases in q and r_1. T_1-weighted phantom images establish that the CG sensors are capable of visualizing changes in copper levels by MRI at clinical field strengths.

Introduction

Copper is an essential element for life[1−7] in large part because of its ability to cycle between multiple oxidation states. At the same time, this redox reactivity is potentially harmful to living organisms, as compromises in homeostatic control of copper pools can result in oxidative stress and subsequent damage to tissue and organ systems.[8−16] Understanding this dual nature of biological copper has led to our interest in developing new ways to study aspects of copper ion accumulation, trafficking, and export in living systems by molecular imaging, particularly in both of its major oxidation states, Cu^+ and Cu^{2+}.[17−21]

A technique well-suited to this end is magnetic resonance imaging (MRI), a modality that allows noninvasive, three-dimensional visualization of whole organisms with spatial and temporal resolution.[22−29] In this context, paramagnetic metal ions, such as Gd^{3+} ($S = {}^7/_2$), can enhance proton MR signal contrast by increasing the relaxation rates of the protons in water molecules interacting with the metal center. The efficiency with which a contrast agent enhances these rates is called relaxivity (r_1). According to Solomon−Bloembergen−Morgan theory,[30−32] relaxivity values are governed by a variety of factors, including the number of bound water molecules (q), the rotational correlation time (τ_R), and the mean residence lifetime of Gd^{3+}-bound water molecules (τ_M).

As conventional MRI contrast agents exhibit constant r_1 values at a given field, we sought to create complexes whose r_1 values would change in response to Cu^+ and/or Cu^{2+} ions for use as chemosensors. Meade first pioneered this "smart" MRI contrast agent approach for detecting β-galactosidase activity,[33] and several examples of contrast agents that respond to

[†] Department of Chemistry, University of California, Berkeley.
[‡] Howard Hughes Medical Institute, University of California, Berkeley.
[||] University of Torino.
[§] Lawrence Berkeley National Laboratory.

(1) Puig, S.; Thiele, D. J. *Curr. Opin. Chem. Biol.* **2002**, *6*, 171–180.
(2) Prohaska, J. R.; Gybina, A. A. *J. Nutr.* **2004**, *134*, 1003–1006.
(3) Cater, M. A.; Mercer, J. F. B. *Top. Curr. Genet.* **2006**, *14*, 101–129.
(4) Schlief, M.; Gitlin, J. *Mol. Neurobiol.* **2006**, *33*, 81–90.
(5) Maryon, E. B.; Molloy, S. A.; Zimnicka, A. M.; Kaplan, J. H. *BioMetals* **2007**, *20*, 355–364.
(6) Leary, S. C.; Winge, D. R.; Cobine, P. A. *Biochim. Biophys. Acta* **2009**, *1793*, 146–153.
(7) Turski, M. L.; Thiele, D. J. *J. Biol. Chem.* **2009**, *284*, 717–721.
(8) Waggoner, D. J.; Bartnikas, T. B.; Gitlin, J. D. *Neurobiol. Dis.* **1999**, *6*, 221–230.
(9) Bayer, T. A.; Wirths, O.; MajtÈnyi, K.; Hartmann, T.; Multhaup, G.; Beyreuther, K.; Czech, C. *Brain Pathol.* **2001**, *11*, 1–11.
(10) Barnham, K. J.; Masters, C. L.; Bush, A. I. *Nat. Rev. Drug Discovery* **2004**, *3*, 205–214.
(11) Valentine, J. S.; Doucette, P. A.; Potter, S. Z. *Annu. Rev. Biochem.* **2005**, *74*, 563–593.
(12) Culotta, V. C.; Yang, M.; O'Halloran, T. V. *Biochim. Biophys. Acta* **2006**, *1763*, 747–758.
(13) Gaggelli, E.; Kozlowski, H.; Valensin, D.; Valensin, G. *Chem. Rev.* **2006**, *106*, 1995–2044.
(14) Donnelly, P. S.; Xiao, Z.; Wedd, A. G. *Curr. Opin. Chem. Biol.* **2007**, *11*, 128–133.
(15) Millhauser, G. L. *Annu. Rev. Phys. Chem.* **2007**, *58*, 299–320.
(16) Davies, P.; Brown, D. R. *Biochem. J.* **2008**, *410*, 237–244.
(17) Zeng, L.; Miller, E. W.; Pralle, A.; Isacoff, E. Y.; Chang, C. J. *J. Am. Chem. Soc.* **2006**, *128*, 10–11.
(18) Miller, E. W.; Zeng, L.; Domaille, D. W.; Chang, C. J. *Nat. Protocols* **2006**, *1*, 824–827.
(19) Que, E. L.; Chang, C. J. *J. Am. Chem. Soc.* **2006**, *128*, 15942–15943.

enzymatic activity,[33−45] pH,[46−52] glucose,[53,54] lactate,[55] nitric oxide,[56] Ca^{2+},[57−63] Zn^{2+},[64−69] and K^{+}[70] have also been described. We recently reported the synthesis and properties of Copper-Gad-1 (CG1),[19] the first copper-activated MR sensor. This initial design was capable of sensing changes in Cu^{2+} levels in aqueous solution with good selectivity over abundant cellular cations but exhibited a modest turn-on change (a 41% increase) that was partially muted in the presence of a 10-fold excess of Zn^{2+}. We have addressed these shortcomings and now present the development of a next-generation family of CG sensors (Figure 1) with greatly improved specificities for Cu^{+} and/or Cu^{2+} ions, particularly over large excesses of Zn^{2+}, with turn-on relaxivity changes of up to 360%. The introduction of thioether-based donors provides a practical strategy for discriminating copper versus zinc ions.[71,72] Included in Figure 2 are CG contrast agents containing copper-binding groups with varied donor atoms (N, S, O) and denticities (3, 4, 5). The copper-induced turn-on responses, binding properties, and metal-ion selectivities of these new CG agents have been investigated using T_1 measurements at 60 MHz. The results of a combination

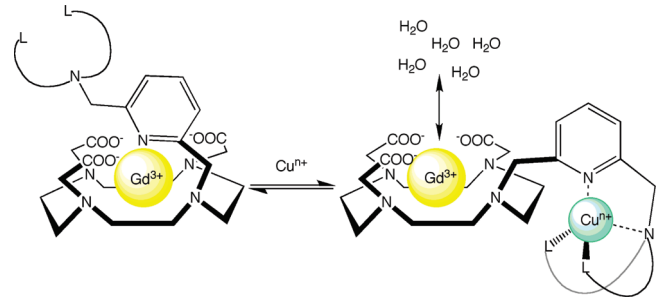

Figure 1. Design strategy for copper-activated MRI sensors.

of nuclear magnetic relaxation dispersion (NMRD) and Dy^{3+}-induced ^{17}O shift (DIS) experiments are consistent with MR-based copper sensing through q modulation. Finally, T_1-weighted phantom images establish that the CG sensors are capable of visualizing changes in copper levels by MRI at clinical field strengths, providing a basis for the potential use of these agents for copper-targeted MRI.

Results and Discussion

Design and Synthesis of Copper-Responsive MRI Contrast Agents. Our approach to creating turn-on, copper-responsive sensors for MRI relies on modulating the relaxivity of a contrast agent by the action of an external trigger, a concept inspired by Meade's original smart contrast agent for β-galactosidase activity.[33] Our first-generation sensor, CG1, combined a DO3A-type Gd^{3+} contrast-agent platform with a pendant iminodiacetate site for binding of Cu^{2+}.[19] Although CG1 was capable of detecting Cu^{2+} ions in aqueous solution at physiological pH,

(20) Domaille, D. W.; Que, E. L.; Chang, C. J. *Nat. Chem. Biol.* **2008**, *4*, 168–175.
(21) Que, E. L.; Domaille, D. W.; Chang, C. J. *Chem. Rev.* **2008**, *108*, 1517–1549.
(22) Aime, S.; Fasano, M.; Terreno, E. *Chem. Soc. Rev.* **1998**, *27*, 19–29.
(23) Caravan, P.; Ellison, J. J.; McMurry, T. J.; Lauffer, R. B. *Chem. Rev.* **1999**, *99*, 2293–2352.
(24) Tóth, É.; Burai, L. s.; Merbach, A. E. *Coord. Chem. Rev.* **2001**, *216−217*, 363–382.
(25) Aime, S.; Botta, M.; Terreno, E. *Adv. Inorg. Chem.* **2005**, *57*, 173–238.
(26) Raymond, K. N.; Pierre, V. C. *Bioconjugate Chem.* **2005**, *16*, 3–8.
(27) Bünzli, J.-C. G. *Acc. Chem. Res.* **2006**, *39*, 53–61.
(28) Woods, M.; Woessner, D. E.; Sherry, A. D. *Chem. Soc. Rev.* **2006**, *35*, 500–511.
(29) Werner, E. J.; Datta, A.; Jocher, C. J.; Raymond, K. N. *Angew. Chem., Int. Ed.* **2008**, *47*, 2–15.
(30) Solomon, I. *Phys. Rev.* **1955**, *99*, 559–565.
(31) Bloembergen, N. *J. Chem. Phys.* **1957**, *27*, 572–573.
(32) Bloembergen, N.; Morgan, L. O. *J. Chem. Phys.* **1961**, *34*, 842–850.
(33) Moats, R. A.; Fraser, S. E.; Meade, T. J. *Angew. Chem., Int. Ed. Engl.* **1997**, *36*, 726–728.
(34) Louie, A. Y.; Hüber, M. M.; Ahrens, E. T.; Rothbächer, U.; Moats, R.; Jacobs, R. E.; Fraser, S. E.; Meade, T. J. *Nat. Biotechnol.* **2000**, *18*, 321–325.
(35) Nivorozhkin, A. L.; Kolodziej, A. F.; Caravan, P.; Greenfield, M. T.; Lauffer, R. B.; McMurry, T. J. *Angew. Chem., Int. Ed.* **2001**, *40*, 2903–2906.
(36) Zhao, M.; Josephson, L.; Tang, Y.; Weissleder, R. *Angew. Chem., Int. Ed.* **2003**, *42*, 1375–1378.
(37) Duimstra, J. A.; Femia, F. J.; Meade, T. J. *J. Am. Chem. Soc.* **2005**, *127*, 12847–12855.
(38) Querol, M.; Chen, J. W.; Weissleder, R.; Bogdanov, A. *Org. Lett.* **2005**, *7*, 1719–1722.
(39) Wei, Q.; Seward, G. K.; Hill, P. A.; Patton, B.; Dimitrov, I. E.; Kuzma, N. N.; Dmochowski, I. J. *J. Am. Chem. Soc.* **2006**, *128*, 13274–13283.
(40) Yoo, B.; Pagel, M. D. *J. Am. Chem. Soc.* **2006**, *128*, 14032–14033.
(41) Giardiello, M.; Lowe, M. P.; Botta, M. *Chem. Commun.* **2007**, 4044–4046.
(42) Breckwoldt, M. O.; Chen, J. W.; Stangenberg, L.; Aikawa, E.; Rodriguez, E.; Qiu, S.; Moskowitz, M. A.; Weissleder, R. *Proc. Natl. Acad. Sci. U.S.A.* **2008**, *105*, 18584–18589.
(43) Chauvin, T.; Durand, P.; Bernier, M.; Meudal, H.; Doan, B.-T.; Noury, F.; Badet, B.; Beloeil, J.-C.; Tóth, É. *Angew. Chem., Int. Ed.* **2008**, *47*, 4370–4372.
(44) Hanaoka, K.; Kikuchi, K.; Terai, T.; Komatsu, T.; Nagano, T. *Chem.−Eur. J.* **2008**, *14*, 987–995.
(45) Mizukami, S.; Takikawa, R.; Sugihara, F.; Hori, Y.; Tochio, H.; Walchli, M.; Shirakawa, M.; Kikuchi, K. *J. Am. Chem. Soc.* **2008**, *130*, 794–795.
(46) Hall, J.; Häner, R.; Aime, S.; Botta, M.; Faulkner, S.; Parker, D.; Sousa, A. S. *New J. Chem.* **1998**, *22*, 627–631.
(47) Aime, S.; Crich, S. G.; Botta, M.; Giovenzana, G.; Palmisano, G.; Sisti, M. *Chem. Commun.* **1999**, 1577–1578.
(48) Zhang, S.; Wu, K.; Sherry, A. D. *Angew. Chem., Int. Ed.* **1999**, *38*, 3192–3194.
(49) Lowe, M. P.; Parker, D.; Reany, O.; Aime, S.; Botta, M.; Castellano, G.; Gianolio, E.; Pagliarin, R. *J. Am. Chem. Soc.* **2001**, *123*, 7601–7609.
(50) Aime, S.; Castelli, D. D.; Terreno, E. *Angew. Chem., Int. Ed.* **2002**, *41*, 4334–4336.
(51) Woods, M.; Kiefer, G. E.; Bott, S.; Castillo-Muzquiz, A.; Eshelbrenner, C.; Michaudet, L.; McMillan, K.; Mudigunda, S. D. K.; Ogrin, D.; Tircso, G.; Zhang, S.; Zhao, P.; Sherry, A. D. *J. Am. Chem. Soc.* **2004**, *126*, 9248–9256.
(52) Tóth, É.; Bolskar, R. D.; Borel, A.; Gonzalez, G.; Helm, L.; Merbach, A. E.; Sitharaman, B.; Wilson, L. J. *J. Am. Chem. Soc.* **2005**, *127*, 799–805.
(53) Zhang, S.; Trokowski, R.; Sherry, A. D. *J. Am. Chem. Soc.* **2003**, *125*, 15288–15289.
(54) Trokowski, R.; Zhang, S.; Sherry, A. D. *Bioconjugate Chem.* **2004**, *15*, 1431–1440.
(55) Aime, S.; Delli Castelli, D.; Fedeli, F.; Terreno, E. *J. Am. Chem. Soc.* **2002**, *124*, 9364–9365.
(56) Liu, G.; Li, Y.; Pagel, M. D. *Magn. Reson. Med.* **2007**, *58*, 1249–1256.
(57) Li, W.-H.; Fraser, S. E.; Meade, T. J. *J. Am. Chem. Soc.* **1999**, *121*, 1413–1414.
(58) Li, W.-H.; Parigi, G.; Fragai, M.; Luchinat, C.; Meade, T. J. *Inorg. Chem.* **2002**, *41*, 4018–4024.
(59) Atanasijevic, T.; Shusteff, M.; Fam, P.; Jasanoff, A. *Proc. Natl. Acad. Sci. U.S.A.* **2006**, *103*, 14707–14712.
(60) Angelovski, G.; Fouskova, P.; Mamedov, I.; Canals, S.; Tóth, É.; Logothetis, N. K. *ChemBioChem* **2008**, *9*, 1729–1734.
(61) Dhingra, K.; Fousková, P.; Angelovski, G.; Maier, M.; Logothetis, N.; Tóth, É. *J. Biol. Inorg. Chem.* **2008**, *13*, 35–46.
(62) Dhingra, K.; Maier, M. E.; Beyerlein, M.; Angelovski, G.; Logothetis, N. K. *Chem. Commun.* **2008**, 3444–3446.
(63) Mishra, A.; Fousková, P.; Angelovski, G.; Balogh, E.; Mishra, A. K.; Logothetis, N. K.; Tóth, É. *Inorg. Chem.* **2008**, *47*, 1370–1381.
(64) Hanaoka, K.; Kikuchi, K.; Urano, Y.; Nagano, T. *J. Chem. Soc., Perkin Trans.* **2001**, 1840–1843.

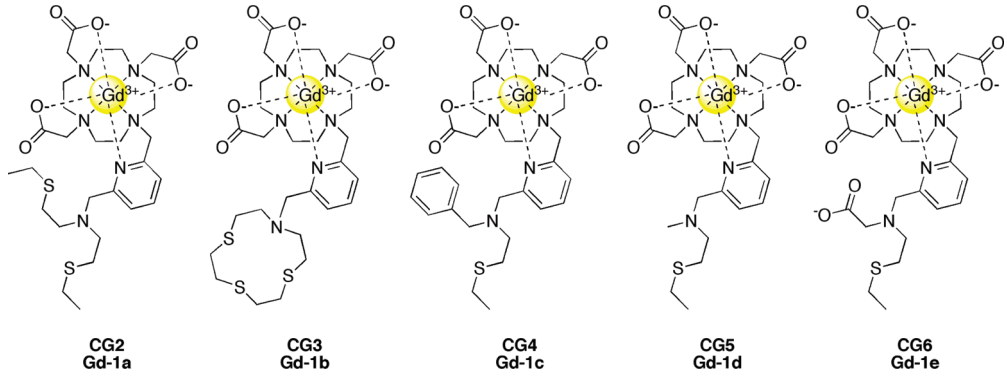

Figure 2. Thioether-based Copper-Gad (CG) contrast-agent platforms.

Scheme 1. General Synthetic Route to MR Sensors CG2−CG6

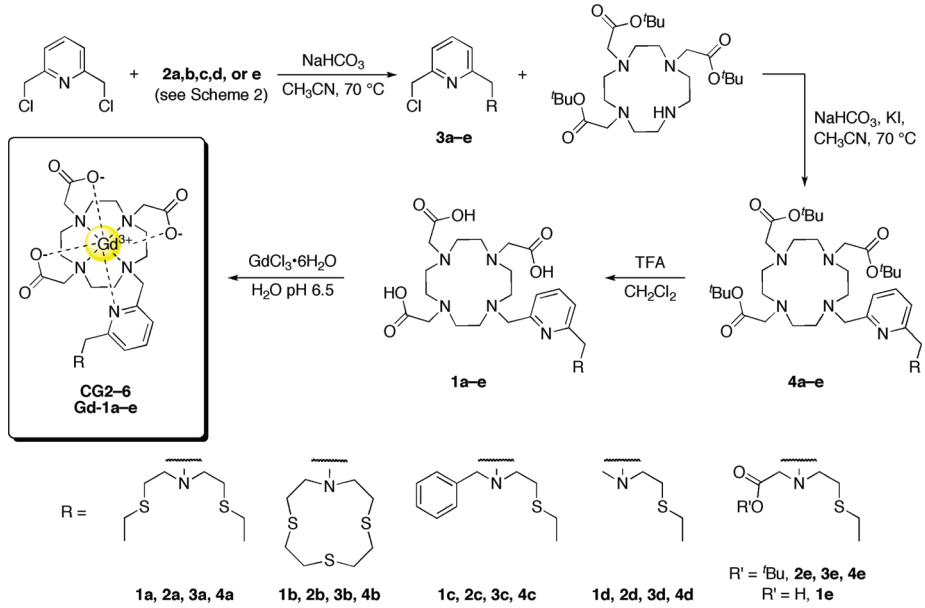

limitations of this initial CG1 design included a relatively modest turn-on response to Cu^{2+} in PBS or HEPES buffer (a 41% increase) and a partially disrupted Cu^{2+} response in the presence of a 10-fold excess of Zn^{2+}. We therefore sought to develop copper-activated MR sensors with improved selectivity, particularly over Zn^{2+}, as well as agents that exhibit a greater sensitivity and change in relaxivity upon binding of copper ions. In addition, we also targeted agents that would be activated by Cu^{+} and/or Cu^{2+} in order to potentially track copper in either of its major oxidation states in biological systems. To achieve this goal, we appended various thioether-based copper receptors to a Gd^{3+}−DO3A scaffold through a 2,6-dimethylpyridine linker switch. We reasoned that in the absence of copper ions, the pyridyl linker would cap the DO3A unit, limit inner-sphere access of water ligands to the Gd^{3+} center, and therefore minimize proton relaxivity. Binding of Cu^{+} and/or Cu^{2+} to the pyridyl-functionalized thioether receptors would reduce the steric bulk around the Gd^{3+} center, affording greater inner-sphere water access to the f^7 metal ion and an increase in relaxivity.

The general synthetic route to a series of new copper-sensing MRI contrast agents is outlined in Scheme 1. The modular synthetic strategy used to obtain Copper-Gad probes 2−6 (CG2−CG6) allowed facile tuning of the metal-binding properties by incorporation of a variety of aminothioether groups into the sensor portion of the contrast-agent platform. The secondary amine building blocks **2a**−**e** were prepared as shown in Scheme 2. Bis(2-(ethylthio)ethyl)amine (**2a**)[73] and 1,4,7-trithia-10-

(65) Hanaoka, K.; Kikuchi, K.; Urano, Y.; Narazaki, M.; Yokawa, T.; Sakamoto, S.; Yamaguchi, K.; Nagano, T. *Chem. Biol.* **2002**, *9*, 1027–1032.
(66) Trokowski, R.; Ren, J.; Kálmán, F. K.; Sherry, A. D. *Angew. Chem., Int. Ed.* **2005**, *44*, 6920–6923.
(67) Major, J. L.; Parigi, G.; Luchinat, C.; Meade, T. J. *Proc. Natl. Acad. Sci. U.S.A.* **2007**, *104*, 13881–13886.
(68) Zhang, X.; Lovejoy, K. S.; Jasanoff, A.; Lippard, S. J. *Proc. Natl. Acad. Sci. U.S.A.* **2007**, *104*, 10780–10785.
(69) Major, J. L.; Boiteau, R. M.; Meade, T. J. *Inorg. Chem.* **2008**, *47*, 10788–10795.
(70) Hifumi, H.; Tanimoto, A.; Citterio, D.; Komatsu, H.; Suzuki, K. *Analyst* **2007**, *132*, 1153–1160.
(71) Cooper, T. H.; Mayer, M. J.; Leung, K. H.; Ochrymowycz, L. A.; Rorabacher, D. B. *Inorg. Chem.* **1992**, *31*, 3796–3804.
(72) Ambundo, E. A.; Deydier, M.-V.; Grall, A. J.; Aguera-Vega, N.; Dressel, L. T.; Cooper, T. H.; Heeg, M. J.; Ochrymowycz, L. A.; Rorabacher, D. B. *Inorg. Chem.* **1999**, *38*, 4233–4242.
(73) Tanaka, M.; Nakamura, M.; Ikeda, T.; Ikeda, K.; Ando, H.; Shibutani, Y.; Yajima, S.; Kimura, K. *J. Org. Chem.* **2001**, *66*, 7008–7012.
(74) Glenny, M. W.; van de Water, L. G. A.; Vere, J. M.; Blake, A. J.; Wilson, C.; Driessen, W. L.; Reedijk, J.; Schröder, M. *Polyhedron* **2006**, *25*, 599–612.
(75) Konrad, M.; Meyer, F.; Heinze, K.; Zsolnai, L. *J. Chem. Soc., Dalton Trans.* **1998**, 199–206.
(76) Nolan, E. M.; Lippard, S. J. *J. Am. Chem. Soc.* **2003**, *125*, 14270–14271.

Scheme 2. Synthesis of Secondary Amine Building Blocks

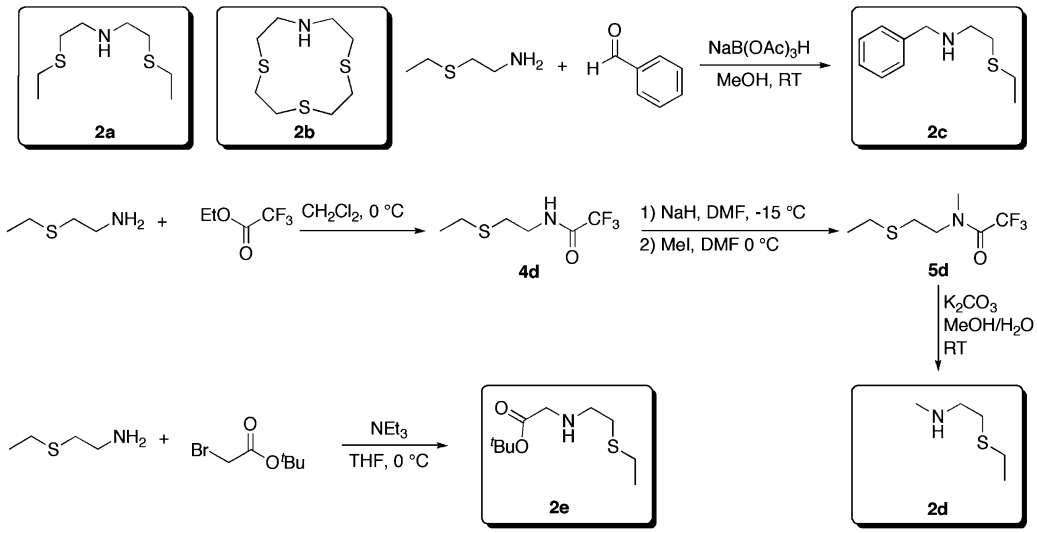

azacyclododecane (**2b**)[74] were synthesized according to literature procedures (for alternative methods, see refs 71 and 75−77). *N*-Benzyl-2-(ethylthio)ethanamine (**2c**), which was previously synthesized from benzylamine,[78] was obtained by reductive amination of benzaldehyde with 2-(ethylthio)ethylamine and sodium triacetoxyborohydride using conditions adapted from the synthesis of a picolyl analogue.[79] We prepared the known compound 2-(ethylthio)-*N*-methylethanamine[80] (**2d**) by an alternative three-step route starting from 2-(ethylthio)ethylamine. First, 2-(ethylthio)ethylamine was reacted with ethyl trifluoroacetate to yield the secondary trifluoroacetamide **4d**. The amide was deprotonated with sodium hydride and alkylated with methyl iodide in a one-pot procedure to yield **5d**. Finally, the secondary amine **2d** was generated in situ using potassium carbonate in 90% methanol/water and used without further purification (see below). *tert*-Butyl 2-(2-(ethylthio)ethylamino)acetate (**2e**) was furnished by reaction of 1 equiv of *tert*-butyl bromoacetate with 2-(ethylthio)ethylamine in the presence of triethylamine.

With the secondary amine precursors in hand, subsequent steps to the final Gd^{3+} contrast agents followed an identical synthetic pathway. First, the reactions of 1 equiv of the secondary amines with 2 equiv of 2,6-bis(chloromethyl)pyridine in dry acetonitrile at 70 °C in the presence of 1 equiv of sodium bicarbonate afforded the desired monochloro compounds **3a**−**e**; employing excess 2,6-bis(chloromethyl)pyridine minimized the formation of the bis-substituted byproduct. DO3A tris(*tert*-butyl ester)[81−83] and **3a**−**e** were then combined in dry acetonitrile with sodium bicarbonate and potassium iodide and reacted at 65 °C for 18−48 h to give the *tert*-butyl-protected ligands **4a**−**e** in a manner similar to that reported by Pope.[84] Cleavage of the *tert*-butyl esters with trifluoroacetic acid (TFA) and purification by reversed-phase HPLC produced the desired ligands **1a**−**e**. The ligands were then metalated with $GdCl_3 \cdot 6H_2O$ in H_2O at pH 6.5 and purified by HPLC to give the final CG contrast agents CG2−CG6 (**Gd**−**1a**−**e**). Notably, HPLC purification ensured the removal of any excess $GdCl_3$. Taken together, the new CG Gd^{3+} complexes CG2−CG6 represent a homologous series of copper-sensing MRI contrast agents bearing a range of thioether-containing receptor components.

(77) Forshee, P. B.; Sibert, J. W. *Synthesis* **2006**, 756–758.
(78) Dawson, T. P. *J. Am. Chem. Soc.* **1933**, *55*, 2070–2075.
(79) Nolan, E. M.; Lippard, S. J. *Inorg. Chem.* **2004**, *43*, 8310–8317.

Table 1. Relaxivity Values of CG2−CG6 at 60 MHz in the Absence and Presence of Cu^+ or Cu^{2+} (r_1), $Cu^{2+/+}$ Reduction Potentials ($E_{1/2}$), and Apparent Dissociation Constants (K_d)

	r_1 (mM^{-1} s^{-1})[a]				
sensor	no Cu	1 equiv of Cu	% increase in r_1	$E_{1/2}$ (V vs SHE)[d]	K_d (M)[e]
CG2	1.5	6.9[b]	360	0.46	2.6×10^{-13} [b]
CG3	1.5	6.9[b]	360	0.58	3.7×10^{-14} [b]
CG4	1.7	6.6[b]	290	0.40	1.4×10^{-11} [b]
CG5	1.2	2.3[b]	92	0.34	3.2×10^{-11} [b]
CG6	2.2	3.8[b,c]	73	0.13	9.9×10^{-16} [c]

[a] Measured in 20 mM HEPES buffer (pH 7) at 37 °C. [b] Using Cu^+. [c] Using Cu^{2+}. [d] Measured in PBS buffer (pH 7.4). [e] Measured in 20 mM HEPES buffer (pH 7) at 25 °C.

Turn-On Relaxivity Responses to Copper Ions and Electrochemistry. The longitudinal relaxivity values for the CG contrast agents in the absence or presence of copper ions were determined using T_1 measurements at 60 MHz. The studies were performed at 37 °C in 20 mM HEPES buffer (pH 7), and the solutions of the purified CG sensors used in the relaxivity experiments contained 0.2 mM Gd^{3+} as determined by ICP−OES. The spectroscopic data are collected in Table 1.

In the absence of added copper ions, the five Gd^{3+} complexes in the series exhibited relaxivities ranging from 1.2 mM^{-1} s^{-1} (for CG5) to 2.2 mM^{-1} s^{-1} (for CG6). The low observed relaxivity values are consistent with Gd^{3+} complexes possessing limited inner-sphere water access ($q = 0$), suggesting that the pyridine linker effectively caps the paramagnetic Gd^{3+} center in the absence of competing metal ions. Although the CG ligand framework contains eight atoms for lanthanide chelation, leaving one potential open site for water binding, a comparable Eu^{3+} complex containing a methyldipicolylamine substituent at the 6-position of the pyridine cap also contained zero inner-sphere water molecules, as determined by luminescence lifetime measurements.[84] The steric contribution of bulky substituents at the 6-position of the pyridine cap is evident, as a similar Gd^{3+} complex containing a pyridine cap with only a hydrogen group at the 6-position possessed one inner-sphere water molecule and exhibited a relaxivity of 5.3 mM^{-1} s^{-1} at 20 MHz.[85] The small variation in relaxivity values for CG2−CG6 may be due to contributions from outside the first coordination sphere of these complexes. NMRD experiments provided supporting evidence for this proposal (see below).

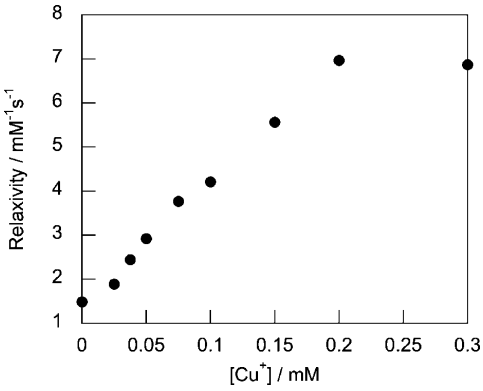

Figure 3. Relaxivity response of 0.2 mM CG2 to various concentrations of Cu^+. Relaxivity measurements were performed at 37 °C in 20 mM HEPES buffer (pH 7) at a proton Larmor frequency of 60 MHz.

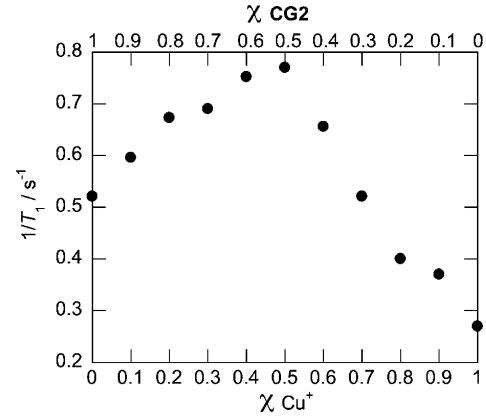

Figure 4. Job's plot for CG2 and Cu^+. The total concentrations of CG2 and Cu^+ were kept constant at 0.2 mM. Relaxivity measurements were performed at 37 °C in 20 mM HEPES buffer (pH 7) at a proton Larmor frequency of 60 MHz. The maximum responses at a mole fraction of 0.5 for both CG2 and Cu^+ is consistent with formation of a 1:1 Cu^+/CG2 complex.

Upon addition of up to 1 equiv of copper ions, the relaxivity values of the CG contrast agents increased, establishing the ability of these probes to sense copper using the MR modality (Table 1, Figure 3). CG2, CG3, CG4, and CG5 responded to Cu^+ with relaxivity increases ranging from 92% to 360%. CG2 and CG3 exhibited the greatest turn-on responses, as their r_1 values increased from 1.5 mM^{-1} s^{-1} in the absence of Cu^+ to 6.9 mM^{-1} s^{-1} upon Cu^+ binding (a 360% increase). These values represent the largest relaxivity enhancements observed to date for metal-activated MRI contrast agents and a ~9-fold improvement in copper ion response relative to that for CG1 (a 41% increase). The observed difference in the Cu^+ turn-on responses for benzyl-substituted CG4 (a 290% increase) versus methyl-substituted CG5 (a 92% increase), which have the same pyridyl−thioether receptor, show the marked effects that small peripheral substitutions can have on relaxivity properties.

CG6 is a unique member of the CG family that is equally responsive to Cu^+ and Cu^{2+}. Addition of either Cu^+ or Cu^{2+} to CG6 triggered a maximum 73% relaxivity turn-on from r_1 = 2.2 to 3.8 mM^{-1} s^{-1}. Cu^{2+} itself is paramagnetic and has an r_1 value of 1.0 mM^{-1} s^{-1} measured at 10 MHz in water.[86] Under the conditions used for these relaxivity measurements, Cu^{2+} likely does not contribute significantly to the copper-bound CG6 relaxivity, as the relaxivity of $CuSO_4$ in 20 mM HEPES buffer at 60 MHz and 37 °C is <0.1 mM^{-1} s^{-1}. Monitoring the reaction of equimolar amounts of CG6 and Cu^+ by UV−vis absorption spectroscopy revealed that the initial spectrum observed upon mixing quickly (<1 min) evolved into a spectrum identical to that obtained from a 1:1 solution of CG6 and Cu^{2+}, suggesting a redox equilibration for this sensor that favors the higher oxidation state of copper for the N/O/S donor set provided by the pyridyl/carboxylate/thioether receptor. These data were corroborated by the electrochemical Cu^{2+}/Cu^+ reduction potentials measured for the five CG complexes (Table 1). The CG2, CG3, CG4, and CG5 compounds possess very positive Cu^{2+}/Cu^+ redox couples with $E_{1/2}$ values ranging from +0.34 to +0.58 V vs SHE. On the other hand, copper-bound CG6, which responds to both Cu^+ and Cu^{2+}, has the least positive Cu^{2+}/Cu^+ reduction potential at +0.13 V.

The observed relaxivity increases for the CG sensors were stable over time, indicating that the Gd^{3+}−CG complexes remain intact in the presence of $Cu^{+/2+}$. We note that Cu^{2+} can catalyze the dissociation of Gd^{3+}−DTPA in vivo, as the affinities of DTPA for Gd^{3+} and Cu^{2+} are very similar and DTPA is kinetically labile;[87] however, studies with analogous Gd^{3+}−DO3A complexes demonstrated that this ligand is more kinetically inert to metal-ion exchange.[88] To establish the kinetic stability of the CG platforms, we used LC/MS to monitor CG2 in the presence of 1 equiv of Cu^{2+}. No metal-ion exchange was observed at room temperature after 7 days or at 37 °C after 4 h.

Copper Binding Stoichiometries and Affinities. Binding analyses using the method of continuous variations (Job's plot, Figure 4),[89] obtained through T_1 measurements (for CG2 and CG3) or UV−vis absorption measurements (for CG4−CG6), showed inflection points at a mole fraction of 0.5 for both the Gd^{3+} contrast agent and copper ion. Furthermore, plots of relaxivity versus [Cu^{n+}] revealed that the observed relaxivity for a given CG sensor reached a maximum at 1 equiv of Cu^{n+} and leveled off at higher concentrations of added Cu^{n+} (Figure 3). These data are consistent with a 1:1 Cu/CG binding stoichiometry, which was then assumed in all of the K_d calculations.

(80) Demeshko, S.; Leibeling, G.; Maringgele, W.; Meyer, F.; Mennerich, C.; Klauss, H.-H.; Pritzkow, H. *Inorg. Chem.* **2005**, *44*, 519–528.
(81) Li, C.; Wong, W.-T. *Tetrahedron* **2004**, *60*, 5595–5601.
(82) Dadabhoy, A.; Faulkner, S.; Sammes, P. G. *J. Chem. Soc., Perkin Trans.* **2002**, 348–357.
(83) Prasuhn, D. E., Jr.; Yeh, R. M.; Obenaus, A.; Manchester, M.; Finn, M. G. *Chem. Commun.* **2007**, 1269–1271.
(84) Pope, S. J. A.; Laye, R. H. *Dalton Trans.* **2006**, 3108–3113.
(85) Aime, S.; Batsanov, A. S.; Botta, M.; Howard, J. A. K.; Lowe, M. P.; Parker, D. *New J. Chem.* **1999**, *23*, 669–670.
(86) Vymazal, J.; Bulte, J. W. M.; Frank, J. A.; Chiro, G. D.; Brooks, R. A. *J. Magn. Reson. Imaging* **1993**, *3*, 637–640.
(87) Sarka, L.; Burai, L.; Brucher, E. *Chem.—Eur. J.* **2000**, *6*, 719–724.
(88) Tweedle, M. F.; Hagan, J. J.; Kumar, K.; Mantha, S.; Chang, C. A. *Magn. Reson. Imaging* **1991**, *9*, 409–415.
(89) Job, P. *Ann. Chim. (Paris)* **1928**, *9*, 113.
(90) Smith, R. M.; Martell, A. E. *Critical Stability Constants*; Plenum Press: New York, 1989.
(91) Bush, A. I. *Curr. Opin. Chem. Biol.* **2000**, *4*, 184–191.
(92) Frederickson, C. J.; Koh, J. Y.; Bush, A. I. *Nat. Rev. Neurosci.* **2005**, *6*, 449–462.
(93) Chang, C. A.; Francesconi, L. C.; Malley, M. F.; Kumar, K.; Gougoutas, J. Z.; Tweedle, M. F.; Lee, D. W.; Wilson, L. J. *Inorg. Chem.* **1993**, *32*, 3501–3508.
(94) Aime, S.; Gianolio, E.; Terreno, E.; Giovenzana, G. B.; Pagliarin, R.; Sisti, M.; Palmisano, G.; Botta, M.; Lowe, M. P.; Parker, D. *J. Biol. Inorg. Chem.* **2000**, *5*, 488–497.
(95) Urbanczyk-Pearson, L. M.; Femia, F. J.; Smith, J.; Parigi, G.; Duimstra, J. A.; Eckermann, A. L.; Luchinat, C.; Meade, T. J. *Inorg. Chem.* **2008**, *47*, 56–68.

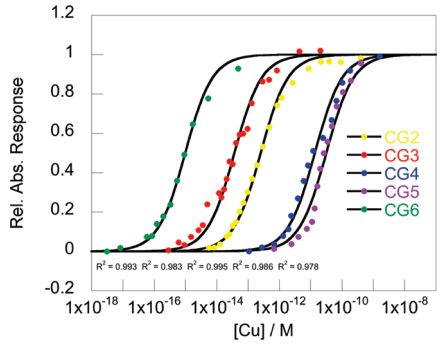

Figure 5. Normalized absorbance responses of 0.2 mM CG2−CG6 to buffered Cu^{+} (CG2−CG5) or Cu^{2+} (CG6) solutions for determination of K_d values. Spectra were acquired in 20 mM HEPES (pH 7). Black lines represent best fits (with each R^2 value displayed below its data set).

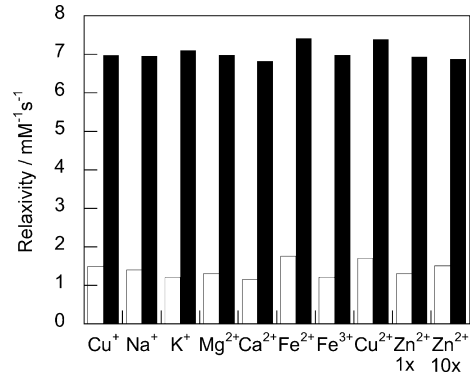

Figure 6. Relaxivity responses of CG2 to various metal ions. White bars represent the addition of an excess of the appropriate metal ion (10 mM for Na^{+}; 2 mM for K^{+}, Mg^{2+}, Ca^{2+}; 0.2 mM for Fe^{2+}, Fe^{3+}, Cu^{2+}) to a 0.2 mM solution of CG2. Response to Zn^{2+} was measured both at 0.2 mM Zn^{2+} (Zn^{2+} 1×) and 2 mM Zn^{2+} (Zn^{2+} 10×). Black bars represent the subsequent addition of 0.2 mM Cu^{+} to the CG2 solution. Relaxivity measurements were acquired at 37 °C in 20 mM HEPES buffer (pH 7) at a proton Larmor frequency of 60 MHz.

Titrations of 0.2 mM solutions of the CG contrast agents with micromolar levels of Cu^{+} or Cu^{2+} ions gave linear responses, indicating that CG2−CG6 bind copper ions tightly, with K_d values $<10^{-6}$ M. The apparent K_d values were obtained by recording changes in the UV−vis absorption spectra of the copper-bound CG contrast agents in the presence of competing ligands with known Cu^{+} (thiourea) or Cu^{2+} (ethylenediamine) affinities (Figure 5).[90] Of the Cu^{+}-responsive MR sensors, CG3, which possesses three thioether donors in an NS_3 macrocycle and five overall potential donor ligands for Cu^{+} binding, exhibited the highest affinity for Cu^{+} ($K_d = 3.7 \times 10^{-14}$ M). The third thioether donor does not appear to play a major role in Cu^{+} binding, as CG2, which contains only two thioether donors and four overall potential donor ligands, coordinated Cu^{+} with a similar affinity ($K_d = 2.6 \times 10^{-13}$ M). The Cu^{+} affinities were further decreased in sensors that provide only three overall potential donor ligands: CG4 and CG5 bind Cu^{+} with observed dissociation constants of $K_d = 1.4 \times 10^{-11}$ and 3.2×10^{-11} M, respectively. The similarity between the K_d values for benzyl-substituted CG4 and methyl-substituted CG5 indicates that the peripheral alkyl pendant does not play a significant role in Cu^{+} binding but markedly affects the relaxivity properties. CG6 binds Cu^{2+} with a much higher affinity ($K_d = 9.9 \times 10^{-16}$ M) than the first-generation CG1 sensor ($K_d = 1.7 \times 10^{-4}$ M).

Selectivity Studies. The CG sensors are highly copper-specific and, in the cases of CG2−CG5, also selective for the Cu^{+} oxidation state, as determined by measuring their relaxivity values in the presence of other competing, biologically relevant metal ions alone or with added copper (Figure 6). These contrast-agent indicators show excellent selectivity for copper ions over abundant cellular alkali and alkaline-earth metal ions at physiological levels: the addition of 10 mM Na^{+}, 2 mM K^{+}, 2 mM Ca^{2+}, or 2 mM Mg^{2+} does not trigger relaxivity enhancements or interfere with copper ion turn-on responses. Likewise, introduction of d-block metal ion competitors, including 0.2 mM Zn^{2+}, 0.2 mM Fe^{2+}, and 0.2 mM Fe^{3+}, does not activate an increase in relaxivity for the CG reagents or greatly affect their ability to sense copper ions.

In particular regard to copper/zinc specificity, a limitation of the original CG1 agent containing an iminodiacetate binding group was a partially muted turn-on response to Cu^{2+} in the presence of large excesses of Zn^{2+}, a situation that can arise in certain biological environments.[10,21,91,92] We therefore tested whether our new thioether-based CG sensors would show improved specificity for copper over this first-generation design. We were delighted to observe that in all cases, turn-on relaxivity responses to $Cu^{+/2+}$ were not affected even in the presence of Zn^{2+} levels at 10-fold excess, and that millimolar concentrations of Zn^{2+} did not give false-positive responses. These data reveal that incorporation of thioether donor ligands into our CG contrast agent scaffolds served not only to increase copper binding affinities but also to tune against Zn^{2+} responses.

The CG series also exhibits redox specificity for copper in both its major oxidation states, Cu^{+} and Cu^{2+}. CG2, CG3, CG4, and CG5 give turn-on relaxivity increases with Cu^{+} but do not respond to Cu^{2+}. Moreover, the presence of Cu^{2+} does not interfere with the Cu^{+}-activated enhancements for these four contrast agents. CG6 responds to both Cu^{+} and Cu^{2+} with the same relaxivity turn-on, whereas CG1 is sensitive only to Cu^{2+} and not Cu^{+}. The potential ability of this new family of CG sensors to sense bioavailable copper pools in either or both of the predominant Cu oxidation states represents a significant advance over the initial CG1 compound.

We also tested the copper responses of CG2−CG6 in the presence of physiologically relevant concentrations of common biological anions (Figure 7). Parker has shown that Gd^{3+}−DO3A-based complexes can bind anions, including phosphate, carbonate, lactate, and citrate,[37,93,94,95] and Eu^{3+}− and Tb^{3+}−DO3A-type complexes have been developed as luminescent anion sensors.[96−102] Phosphate anions do not

(96) Parker, D. *Coord. Chem. Rev.* **2000**, *205*, 109–130.
(97) Bruce, J. I.; Dickins, R. S.; Govenlock, L. J.; Gunnlaugsson, T.; Lopinski, S.; Lowe, M. P.; Parker, D.; Peacock, R. D.; Perry, J. J. B.; Aime, S. *J. Am. Chem. Soc.* **2000**, *122*, 9674–9684.
(98) Lowe, M. P.; Parker, D. *Chem. Commun.* **2000**, 707–708.
(99) Bretonnière, Y.; Cann, M. J.; Parker, D.; Slater, R. *Chem. Commun.* **2002**, 1930–1931.
(100) Atkinson, P.; Bretonnière, Y.; Parker, D. *Chem. Commun.* **2004**, 438–439.
(101) Parker, D.; Yu, J. *Chem. Commun.* **2005**, 3141–3143.
(102) Murray, B. S.; New, E. J.; Pal, R.; Parker, D. *Org. Biomol. Chem.* **2008**, *6*, 2085–2094.
(103) Adrogue, H. J.; Madias, N. E. *N. Engl. J. Med* **1998**, *338*, 26–34.
(104) Lauffer, R. B. *Chem. Rev.* **1987**, *87*, 901–927.
(105) Messeri, D.; Lowe, M. P.; Parker, D.; Botta, M. *Chem. Commun.* **2001**, 2742–2743.
(106) Horrocks, W. D., Jr.; Sudnick, D. R. *Acc. Chem. Res.* **1981**, *14*, 384–392.

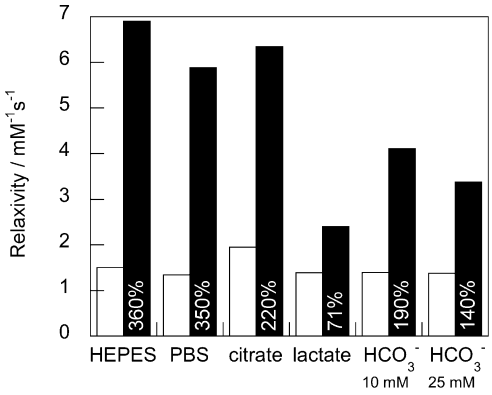

Figure 7. Relaxivity responses of CG2 to 1 equiv of Cu^+ in the presence of biologically relevant anions. White bars represent CG2 relaxivities without Cu^+ in the presence of various anions. Black bars represent CG2 relaxivities with Cu^+ in the presence of different anions. Percentages in the black bars are the % increases in r_1. Relaxivity measurements with HEPES, citrate (0.13 mM), lactate (2.3 mM), and HCO_3^- (10 mM, 25 mM) were acquired at 37 °C in 20 mM HEPES buffer (pH 7) at a proton Larmor frequency of 60 MHz. Relaxivity measurements with PBS were acquired under similar conditions using PBS (pH 7.4).

bind strongly to CG2, as measurements in phosphate-buffered saline (PBS, 10 mM phosphate) revealed a 350% increase in relaxivity in response to Cu^+. Carboxylate-type anions, however, can affect the relaxivity responses of Cu^+-bound CG2. Addition of citrate (0.13 mM) and lactate (2.3 mM) to CG2 resulted in turn-on responses to Cu^+ of 220 and 71%, respectively. Carbonate concentrations also affect the response of CG2: the effect of carbonate was tested at 10 mM $NaHCO_3$ (intracellular)[99] and 25 mM $NaHCO_3$ (extracellular)[103] and gave increases in r_1 in response to Cu^+ of 190 and 140%, respectively. Although the relaxivity increases observed in the presence of anions are still well within a range detectable by MRI,[104] current work is geared toward developing CG sensors with more carboxylate functionalities incorporated into the ligand framework to minimize anion sensitivity.[49,105]

Dysprosium-Induced ^{17}O NMR Shift Experiments. After establishing the ability of the CG sensors to selectively detect Cu^+ and/or Cu^{2+} by changes in longitudinal relaxivity values, we next sought to probe aspects of their mechanism of action. On the basis of our molecular design, we reasoned that the relaxivity differences observed for CG contrast agents in the absence or presence of Cu^+ and/or Cu^{2+} ions are in part due to changes in q, the number of inner-sphere water molecules coordinated to the paramagnetic Gd^{3+} center. Initial experiments to probe this question employed standard luminescence methods developed by Horrocks,[106] but attempts to obtain q by measuring luminescence lifetimes of Eu^{3+} and Tb^{3+} analogues of CG2 in the absence or presence of Cu^+ were unsuccessful, as Cu^+-containing solutions gave luminescence decays that were best fit to multiple lifetimes both in H_2O and D_2O. We suspected that additional quenching pathways beyond those involving inner-sphere H_2O molecules on the lanthanide center may play a role in this system. Cu^+ binding could lead to quenching of the S_1 excited state of the pyridine antenna by electron transfer, thus eliminating energy transfer to the lanthanide ion and the luminescence output. Cu^+ is known to quench the fluorescence of ligands such as bathocuproine disulfonate.[107] In addition, a Eu^{3+} complex containing a phenanthroline unit for metal ion binding experiences quenched emission in the presence of Cu^{2+}.[108]

To circumvent these issues, we turned our attention to an alternative method for obtaining q values, namely, the application of ^{17}O NMR spectroscopy to Dy^{3+} analogues of the CG sensors (DyCG2−DyCG6).[109] Specifically, interactions of water ligands with paramagnetic Dy^{3+} ions lead to an upfield shift of the ^{17}O signals of H_2O in a manner proportional to both the concentration of Dy^{3+} and q. Moreover, this lanthanide-induced shift is largely insensitive to the nonwater ligands coordinated to the paramagnetic metal center.[109] DIS experiments for CG2 and CG3 were performed in 20 mM HEPES buffered at pH 7; CG4 and CG5 spectra were acquired in 10% acetonitrile in 20 mM HEPES buffered at pH 7 because of the solubility and stability of the Cu^+-bound complexes at the higher Dy^{3+} concentrations required for the DIS measurements (1−200 mmol/kg of H_2O). Dy concentrations were calculated using molality (with respect to H_2O) because the ^{17}O shift represents the interaction between Dy^{3+} and H_2O; addition of CH_3CN aids in stabilizing certain complexes but does not affect the DIS. The spectral results were calibrated to a $DyCl_3$ standard (q = 9) to determine the number of bound water molecules for the CG sensors with and without added Cu^+. A plot of DIS versus $DyCl_3$ concentration in HEPES (pH 7) had a slope of 324 ppm/(mol/kg of H_2O), which corresponds to a 36 ppm/(mol/kg of H_2O) shift per bound water molecule. A similar DIS plot for $DyCl_3$ in 10% acetonitrile in 20 mM HEPES (pH 7) exhibited a slope of 362 ppm/(mol/kg of H_2O), which corresponds to 40 ppm/(mol/kg of H_2O) per bound water molecule. Data for DyCG2−DyCG5 are presented in Table 2.

The effects of DyCG2 on the chemical shift of ^{17}O-labeled H_2O were determined in the absence and presence of 1 equiv of Cu^+ at various concentrations of Dy^{3+} (Figure 8). In the absence of Cu^+, the measured ^{17}O shift response for DyCG2 was 9 ppm/(mol/kg H_2O), corresponding to $q = 0.3$. When 1 equiv of Cu^+ was added, the observed shift response increased to 72 ppm/(mol/kg H_2O), corresponding to $q = 2.0$. These data are consistent with the proposal that modulating the number of inner-sphere water molecules plays a role in the copper-activated relaxivity changes exhibited by the CG contrast agents. Similarly, the DyCG3 DIS plot displayed a slope of 11 ppm/(mol/kg H_2O) in the absence of Cu^+, corresponding to $q = 0.3$; addition of 1 equiv of Cu^+ increased the slope to 79 ppm/(mol/kg H_2O), corresponding to $q = 2.2$. DIS measurements on DyCG4 and DyCG5 without Cu^+ yielded slopes of 7 ppm/(mol/kg H_2O) ($q = 0.2$) and 12 ppm/(mol/kg H_2O) ($q = 0.3$), respectively. Cu^+ binding increased the DIS slopes for DyCG4 and DyCG5 to 84 ppm/(mol/kg H_2O) ($q = 2.1$) and 41 ppm/(mol/kg H_2O) ($q = 1.0$), respectively. Notably, direct comparison of the Δq values obtained for DyCG4 and DyCG5 reveals a lower DIS value for the latter, which is consistent with the smaller turn-on increase in r_1 observed for this compound. We were unable to perform meaningful DIS experiments with DyCG6 to determine Δq upon Cu^{2+} binding, as addition of Cu^{2+} led to a downfield shift of the ^{17}O signals of H_2O that counteracted and masked the DIS effect of Dy^{3+}.

(107) Rapisarda, V. A.; Volentini, S. I.; Farìas, R. N.; Massa, E. M. *Anal. Biochem.* **2002**, *307*, 105–109.
(108) Gunnlaugsson, T.; Leonard, J. P.; Senechal, K.; Harte, A. J. *Chem. Commun.* **2004**, 782–783.
(109) Alpoim, M. C.; Urbano, A. M.; Geraldes, C.; Peters, J. A. *J. Chem. Soc., Dalton Trans.* **1992**, 463–467.
(110) Hwang, L.-P.; Freed, J. H. *J. Chem. Phys.* **1975**, *63*, 4017–4025.

Table 2. Estimated q Values for Copper-Sensing MRI Contrast Agents in the Absence and Presence of Copper Ions, As Determined from ^{17}O Dysprosium-Induced Shift (DIS) Measurements

	conditions	slope [ppm/(mol/kg of H_2O)]	q
$DyCl_3$	20 mM HEPES (pH 7)	324	9[a]
$DyCl_3$	10% CH_3CN in 20 mM HEPES (pH 7)	362	9[a]
DyCG2	20 mM HEPES (pH 7)	9	0.3[b]
DyCG2 + Cu^+		72	2[b]
DyCG3	20 mM HEPES (pH 7)	11	0.3[b]
DyCG3 + Cu^+		79	2.2[b]
DyCG4	10% CH_3CN in 20 mM HEPES (pH 7)	7	0.2[c]
DyCG4 + Cu^+		84	2.1[c]
DyCG5	10% CH_3CN in 20 mM HEPES (pH 7)	12	0.3[c]
DyCG5 + Cu^+		41	1.0[c]

[a] See ref 109. [b] Calculated using the value for $q = 9$ $DyCl_3$ in 20 mM HEPES (pH 7). [c] Calculated using the value for $q = 9$ $DyCl_3$ in 10% CH_3CN in 20 mM HEPES (pH 7).

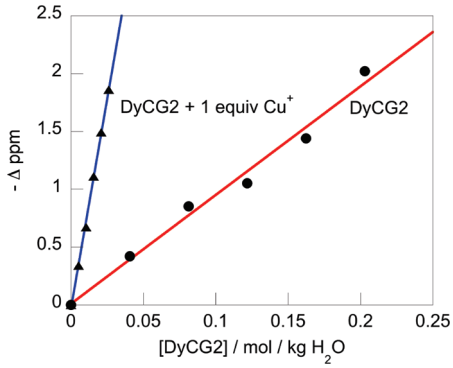

Figure 8. Plot of the DIS of the ^{17}O signal of H_2O ($-\Delta$, in ppm) vs [DyCG2] in the absence (red) and presence (blue) of 1 equiv of Cu^+. Spectra were acquired at room temperature in 20 mM HEPES (pH 7) at an ^{17}O Larmor frequency of 67.8 MHz.

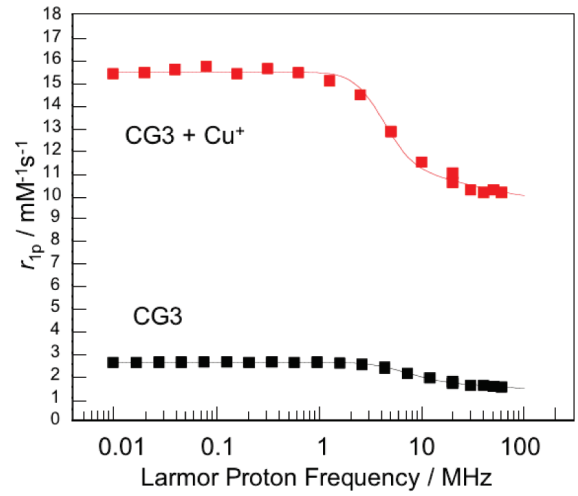

Figure 9. ^1H NMRD profiles of CG3 and CG3 + Cu^+ acquired at 25 °C. The solid lines represent the best-fit profiles.

Nuclear Magnetic Relaxation Dispersion Profiles. As a secondary, independent set of experiments to further probe the mechanisms of copper ion sensing by the CG contrast agents, we also performed NMRD measurements on these sensors in the absence and in the presence of copper ions using a field-cycling relaxometer (Figure 9). The profiles obtained were analyzed using Solomon−Bloembergen−Morgan theory[30−32] for the inner-sphere relaxivity and the Freed model[110] for the outer-sphere relaxivity, with the diffusion coefficient (D) fixed at 2.24×10^5 cm^2 s^{-1}, the distance between Gd^{3+} and the inner-sphere water protons (r) at 3.1 Å, and the inner-sphere exchange lifetime (τ_M) at 160 ns (the reported value for the parent complex Gd^{3+}−DO3A). Profiles were obtained for all compounds in the copper-free state. Profiles in the presence of Cu^{n+} were obtained for CG2−CG4 (Cu^+) and CG6 (Cu^{2+}). For CG5, an NMRD profile could not be obtained for the Cu^+-bound complex because of its low relaxivity and the low solubility of Cu^+ in solution, which resulted in a high degree of error in the measurements. The fitted values are displayed in Table 3.

The NMRD data acquired for the CG series of compounds in the absence of added copper ions are consistent with those for Gd^{3+} contrast agents that do not possess any inner-sphere water molecules. In fact, the measured outer-sphere relaxivities were so low that, in order to obtain a reasonable fit, the distance of closest approach of the outer-sphere water protons (a) was allowed to vary. The distances obtained for the CG complexes (4.2−4.8 Å) were markedly longer than what is observed for typical Gd^{3+} contrast agents with greater water access (3.8−4.0 Å). These values correlate with the copper-free relaxivities of CG2−CG6; longer a values give lower relaxivities and shorter a values give higher relaxivities. For Cu^+-sensing agents CG2−CG4, the estimated change of 2 in q as determined by DIS measurements was also observed in the fitted NMRD data. In fact, any attempt to fit the observed NMRD profiles with $q = 1$ led to very poor agreement between the experimental and calculated values. The change of 1 in q for CG6 upon addition of Cu^{2+} as determined by NMRD is consistent with the lower turn-on response observed for this complex than for CG2−CG4. The reduced q modulation for CG6 relative to CG2−CG4 could indicate that the carboxylic acid moiety used for Cu^{2+} binding also interacts with the Gd^{3+} center in the Cu^{2+}-bound state. The fitted rotational correlation times (τ_R) for copper-bound CG complexes all fall within the range expected for Gd^{3+} complexes with molecular weights of 700−800 Da. Values of τ_R for copper-free CG2−CG6 were fixed close to those for their copper-bound analogues, as fits of NMRD data for $q = 0$ complexes are not sensitive to small changes in τ_R. The values of the average quadratic transient zero-field splitting (Δ^2), the electronic correlation time (τ_v), and the electronic relaxation time at zero field (τ_{s0}), which govern the electronic relaxation time, are relatively similar to each other. These NMRD values are closer to those of Gd^{3+}−DTPA than those of Gd^{3+}−DOTA, reflecting the asymmetry of CG2−CG6.[58]

Table 3. Best-Fit Values to the Solomon−Bloembergen−Morgan Equations for CG2−CG6 in the Absence and Presence of $Cu^{+/2+}$, As Determined from NMRD Experiments[a]

	r_{1p} (mM^{-1} s^{-1} at 20 MHz, 25 °C)	a (Å)	q	τ_R (ps)	Δ^2 (10^{19} s^{-2})	τ_v (ps)	τ_{s0} (ps)
CG2	1.6	4.7 ± 0.11	0[c]	110[d]	5.8 ± 1.1	19 ± 2.4	75.6
CG2 + Cu^+	9.3	3.8[c]	2.00 ± 0.22	110 ± 12.3	5.6 ± 0.4	22 ± 1.4	67.6
CG3	1.6	4.7 ± 0.09	0[c]	130[d]	3.2 ± 0.7	27 ± 4.4	96
CG3 + Cu^+	10.5	3.8[c]	2.03 ± 0.24	128 ± 14.5	2.0 ± 0.6	42 ± 9.2	99
CG4	2.1	4.2 ± 0.15	0[c]	130[d]	3.4 ± 1.4	25 ± 7.7	99
CG4 + Cu^+	10.4	3.8[c]	2.06 ± 0.26	128 ± 15.5	2.5 ± 0.8	37 ± 8.1	90
CG5	1.6	4.8 ± 0.12	0[c]	100[e]	3.5 ± 0.8	25 ± 4.2	95
CG5 + Cu^+ [b]	–	–	–	–	–	–	–
CG6	2.2	4.2 ± 0.13	0[c]	80[d]	8.4 ± 2.0	16 ± 2.7	61
CG6 + Cu^{2+}	4.8	3.8[c]	1 ± 0.18	78 ± 2.9	5.4 ± 0.6	17 ± 1.6	90

[a] Measurements were performed at 25 °C in 20 mM HEPES (pH 7). Relaxivity values for copper-free CG2−CG6 and CG6 + Cu^{2+} were measured at 0.5 mM concentration. Cu^+-containing solutions were measured at 0.1 mM because of the low solubility of Cu^+ in aqueous solution. The contribution to the observed relaxivity by Cu^{2+} was included in the outer-sphere term but is likely to be negligible. [b] Relaxivity too low to perform NMRD measurements at 0.1 mM concentration. [c] Fixed in the fitting procedure. [d] Values were not experimentally determined and were assumed to be equal to the corresponding $q \neq 0$ complexes. [e] Given the similarity of the structures of CG2−CG6, the τ_R value for CG5 was set to the average τ_R value of the other complexes.

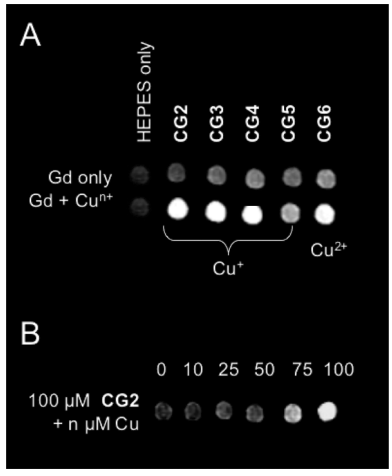

Figure 10. (A) T_1-weighted phantom images of 100 μM CG2−CG6 in 20 mM HEPES (pH 7) with and without 1 equiv of Cu^{n+}. (B) Phantom images of 100 μM CG2 with 0, 10, 25, 50, 75, and 100 μM $[Cu(NCCH_3)_4]PF_6$. Images were acquired at 25 °C at 1.5 T (~64 MHz proton Larmor frequency).

Copper-Activated T_1-Weighted Phantom Magnetic Resonance Imaging. With spectroscopic data showing the turn-on relaxivity responses, binding properties, metal ion selectivities, and copper-induced changes in q values for this new series of CG contrast agents in hand, we next sought to test the ability of these sensors to detect changes in aqueous Cu^+ and/or Cu^{2+} levels using MRI. To demonstrate the potential feasibility of these MR sensors for molecular-imaging applications, we acquired T_1-weighted images of the CG complexes in the absence and the presence of copper ions with a commercial 1.5 T magnet (Avanto Siemens MRI system). The phantom MR images depicted in Figure 10A show that all of the CG sensors can detect contrast between samples with and without added copper ions at clinically relevant field strengths. Moreover, images of 100 μM CG2 with Cu^+ added at concentrations of 0, 10, 25, 50, 75, and 100 μM (Figure 10B) reveal that this MR probe can readily visualize differences in copper levels in a biologically relevant micromolar range, given a known contrast agent concentration. In this context, chelatable copper pools have been identified in the mitochondrial matrix[111] and in the Golgi apparatus.[112] Moreover, the cerebrospinal fluid (CSF) contains micromolar levels of copper ion, most of which is not bound to ceruloplasmin because of the low concentrations of this protein in the CSF;[113,114] this may result in facile exchange between different copper binding ligands.[115]

Concluding Remarks

In summary, we have described the design, synthesis, and evaluation of a new family of copper-activated MR contrast agents. The Copper-Gad sensors combine a Gd^{3+}−DO3A core with various thioether-based copper receptor switches to give marked increases in longitudinal relaxivity in response to either Cu^+ or Cu^{2+}, with turn-on responses up to 360%, as well as high selectivity for Cu^+ and/or Cu^{2+} over competing metal ions at cellular concentrations. A combination of ^{17}O NMR DIS and NMRD measurements supports a mechanism in which the observed turn-on relaxivity responses involve copper-induced changes in the coordination environment of the Gd^{3+} core that result in an increase in q. T_1-weighted phantom images have established that the CG sensors are capable of visualizing changes in copper levels by MRI at clinical field strengths. The new contrast agents CG2−CG6 show significant gains in selectivity, sensitivity, and turn-on response over the first-generation CG1 construct. In particular, the use of thioether-based receptors provides a practical strategy for obtaining superior selectivity for copper over zinc ions. Whereas the original CG1 compound showed a partially muted turn-on response to Cu^{2+} in the presence of a 10-fold excess of Zn^{2+}, the copper-induced relaxivity increases for the new CG sensors are unaffected by large excesses of zinc ions. Oxidation-state specificity for Cu^+ has also been obtained by the use of neutral donor sets bearing thioether ligands, providing an entry into sensors that can distinguish Cu^+ and Cu^{2+}. In terms of sensitivity and turn-on response, the relaxivity enhancements for CG2 and CG3

(111) Cobine, P. A.; Ojeda, L. D.; Rigby, K. M.; Winge, D. R. *J. Biol. Chem.* **2004**, *279*, 14447–14455.
(112) Yang, L. C.; McRae, R.; Henary, M. M.; Patel, R.; Lai, B.; Vogt, S.; Fahrni, C. J. *Proc. Natl. Acad. Sci. U.S.A.* **2005**, *102*, 11179–11184.
(113) Weisner, B.; Hartard, C.; Dieu, C. *J. Neurol. Sci.* **1987**, *79*, 229–237.
(114) Hartard, C.; Weisner, B.; Dieu, C.; Kunze, K. *J. Neurol.* **1993**, *241*, 101–107.
(115) Peña, M. M. O.; Lee, J.; Thiele, D. J. *J. Nutr.* **1999**, *129*, 1251–1260.

are almost an order of magnitude greater than that observed for CG1 (360% versus 41%). Taken together, these results establish an approach to selective, sensitive detection of copper through MRI. Current work is focused on the application of these CG sensors and development of next-generation analogues for studies of copper physiology and pathology using MR-based molecular imaging.

Acknowledgment. We thank the University of California, Berkeley, the Dreyfus, Beckman, Packard, and Sloan Foundations, the Hellman Faculty Fund (UC Berkeley), the National Institute of General Medical Sciences (NIH GM 79465), and the Howard Hughes Medical Institute for funding this work. We thank Ms. Christine Yin for preliminary synthetic studies. E.L.Q. acknowledges a Branch Graduate Fellowship from UC Berkeley.

Supporting Information Available: Synthetic and spectroscopic experimental procedures and additional data for CG2−CG6 not presented in the main text. This material is available free of charge via the Internet at http://pubs.acs.org.

JA900884J